Visible-light orbital phase curves: A two-front effort

Avi Shporer
Sagan Fellow, JPL

Sagan Fellows Symposium 5.8.2015

Photometric variability correlated with the orbit:

Loeb & Gaudi 2003, Jenkins & Doyle 2003, Zucker et al. 2007, Pfahl et al. 2008, Faigler & Mazeh 2011, Shporer et al. 2011

Gravitational: •Beaming
•Tidal deformation

Atmospheric: Reflection + Heating

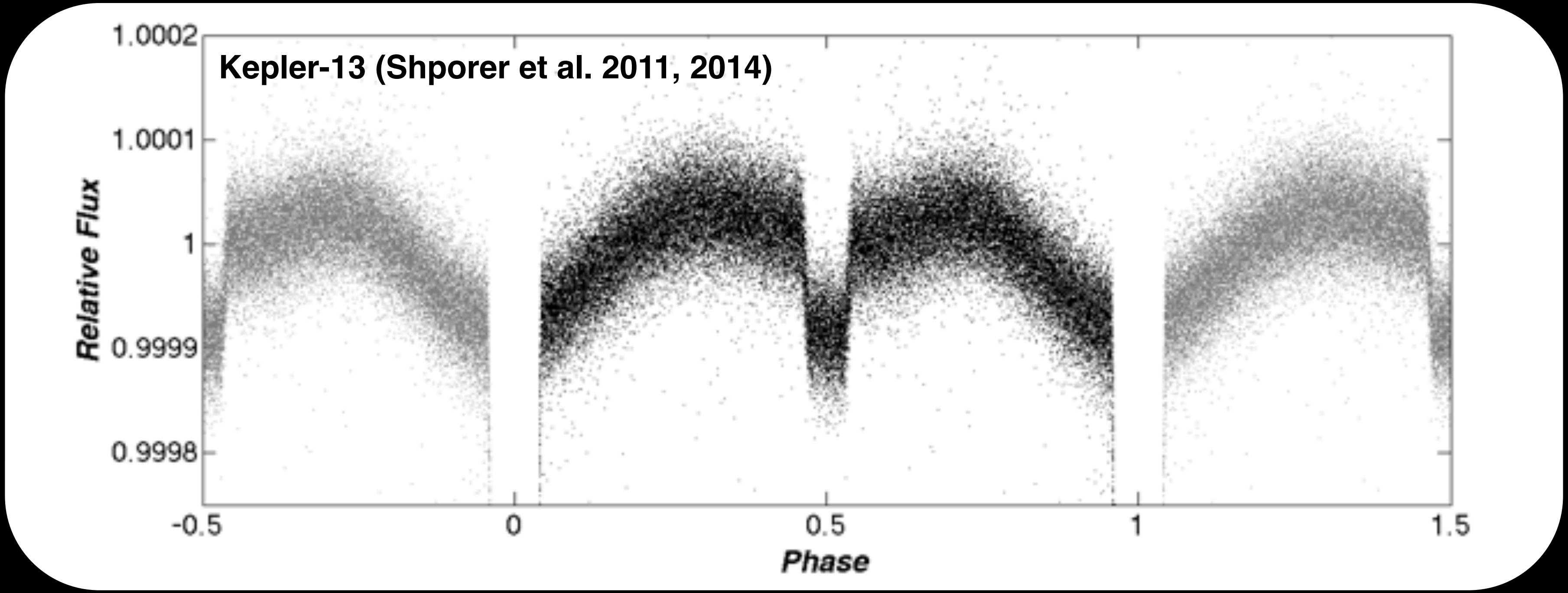

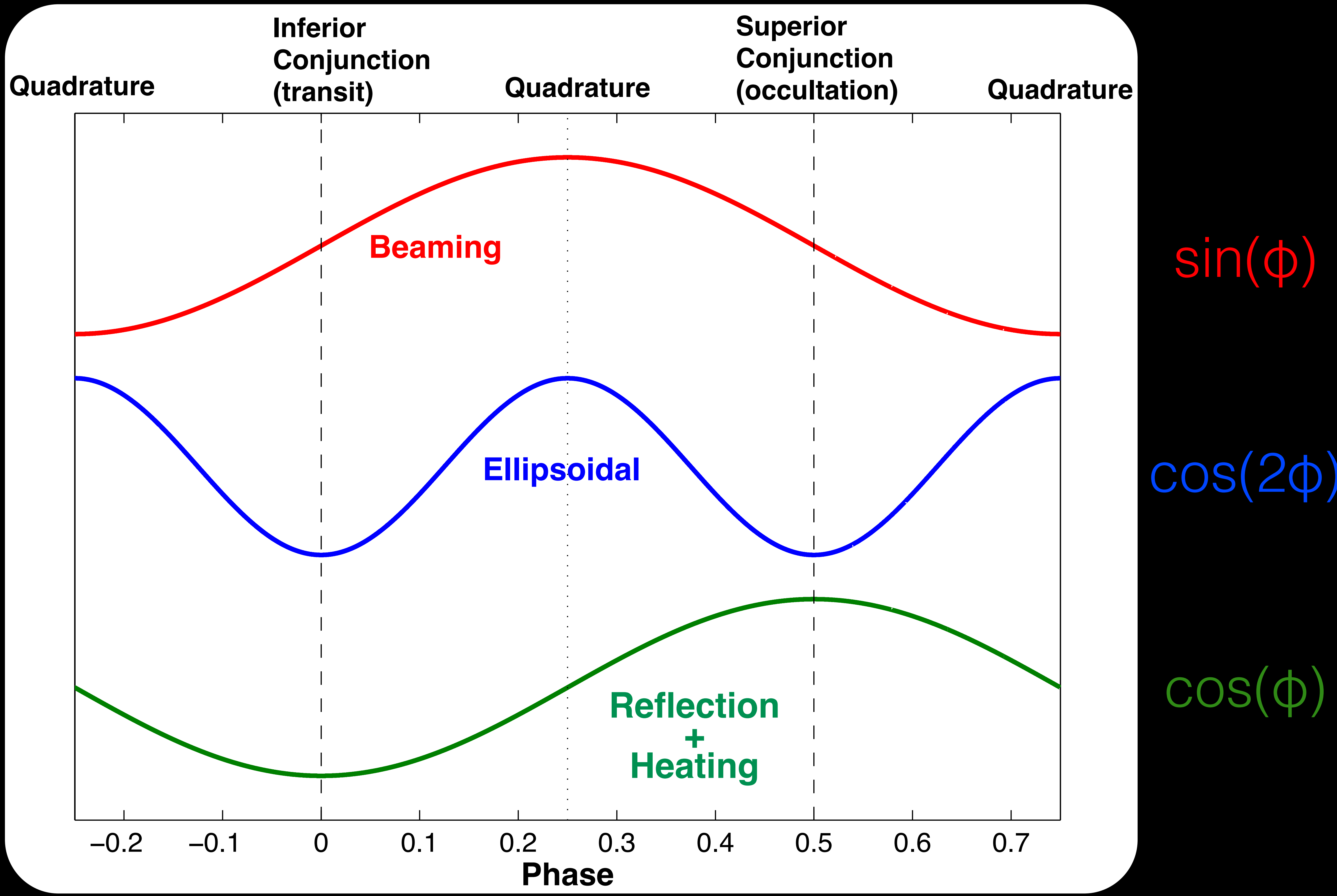

Unique period+phase for each component

Gravitational

Beaming

$$A_{\mathrm{beam}} = \alpha_{\mathrm{beam}} \frac{4}{c} \frac{M_2 \sin i}{(M_s + M_2)^{2/3}} \left(\frac{2\pi G}{P} \right)^{1/3}$$

Tidal Ellipsoidal Deformation

$$A_{\mathrm{ellip}} = \alpha_{\mathrm{ellip}} \frac{M_2 \sin^2 i}{M_s} \left(\frac{R_s}{a} \right)^3$$

Atmospheric

Reflection+heating

$$A_{\mathrm{refl}} = \alpha_{\mathrm{refl}} 0.1 \left(\frac{R_2}{a} \right)^2 \sin i$$

Two-Front Effort

Detailed study:
- Atmosphere
- Ellipsoidal distortion

Orbital phase curves

Detection Method, rare systems:
- Non-eclipsing
- Large sample

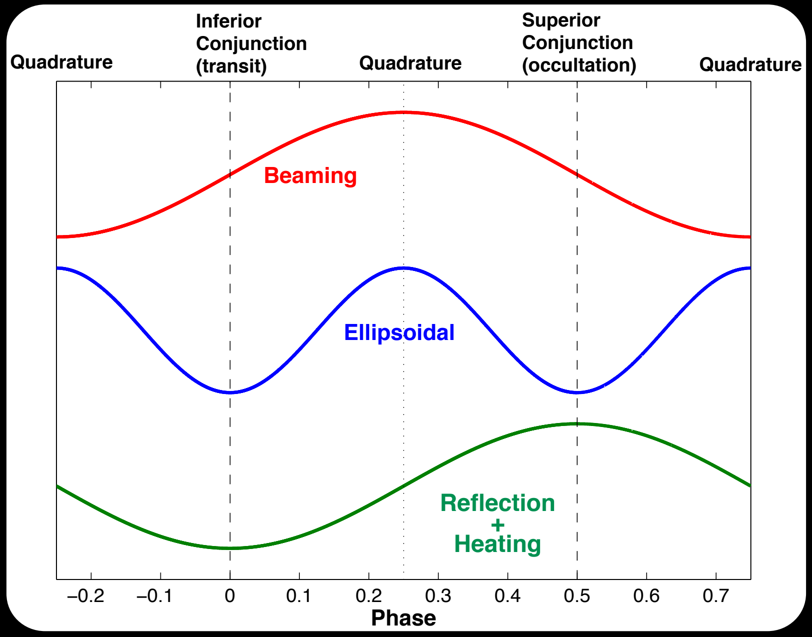

Is it really that simple?

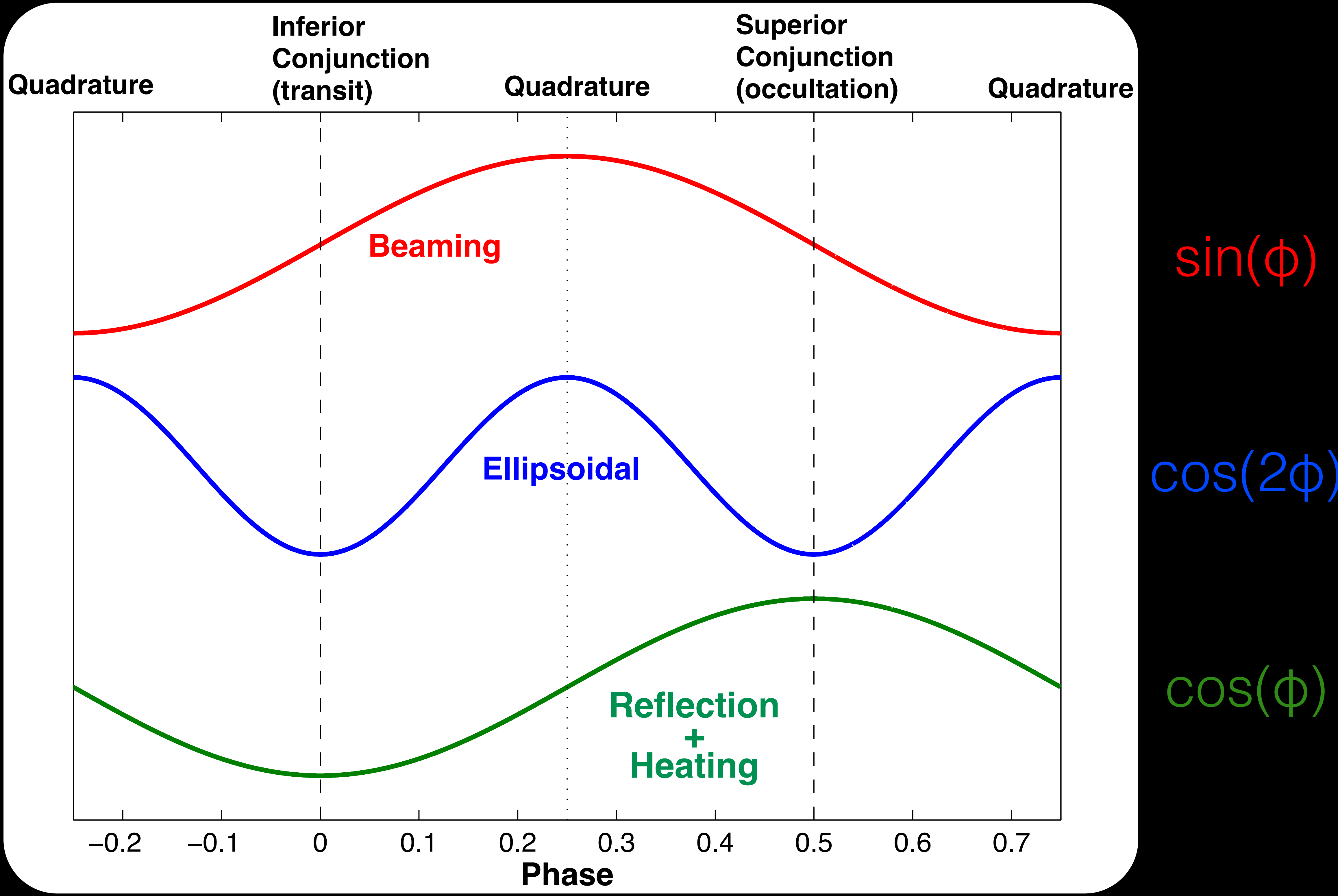

Unique period+phase for each component

Atmosphere-dominated *kepler* phase curves

Shporer & Hu 2015, arXiv:1504.00498

Kepler confirmed transiting planets:

- Detectable phase curve
- No gravitational effects

⇨ “clear view” of the atmosphere

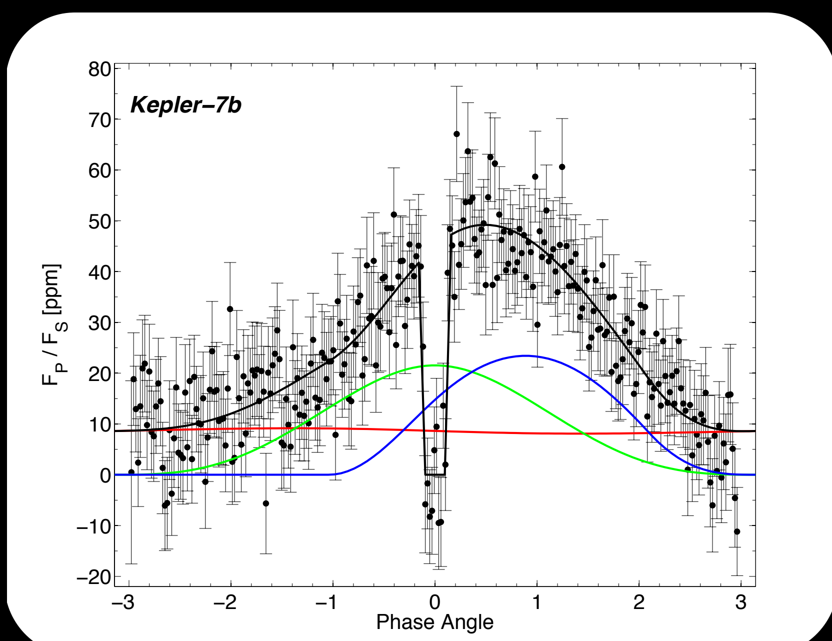

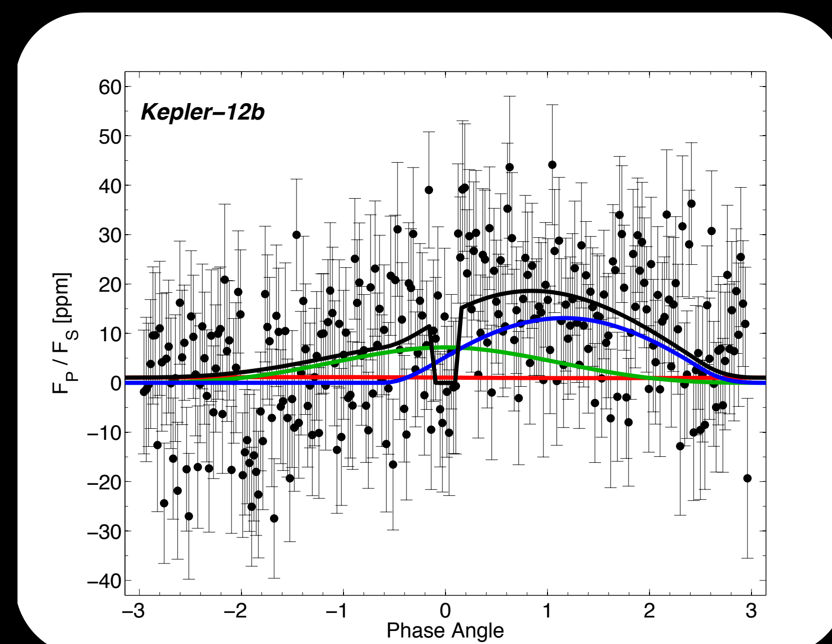

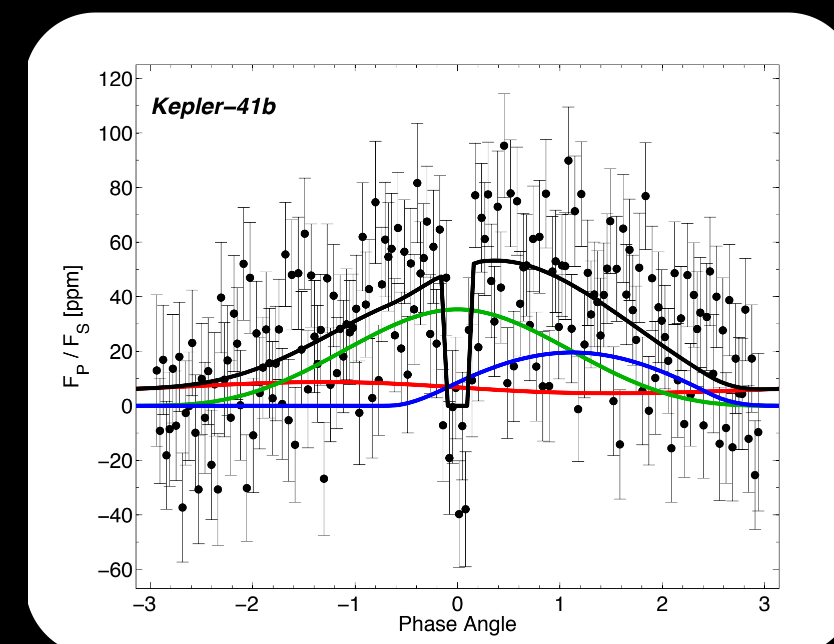

See also: Demory et al. 2013,
Hu et al. 2015

Post-occultation maximum

Atmosphere-dominated *kepler* phase curves

Shporer & Hu 2015

Kepler confirmed transiting planets:

- Detectable phase curve
- No gravitational effects

⇒ "clear view" of the atmosphere

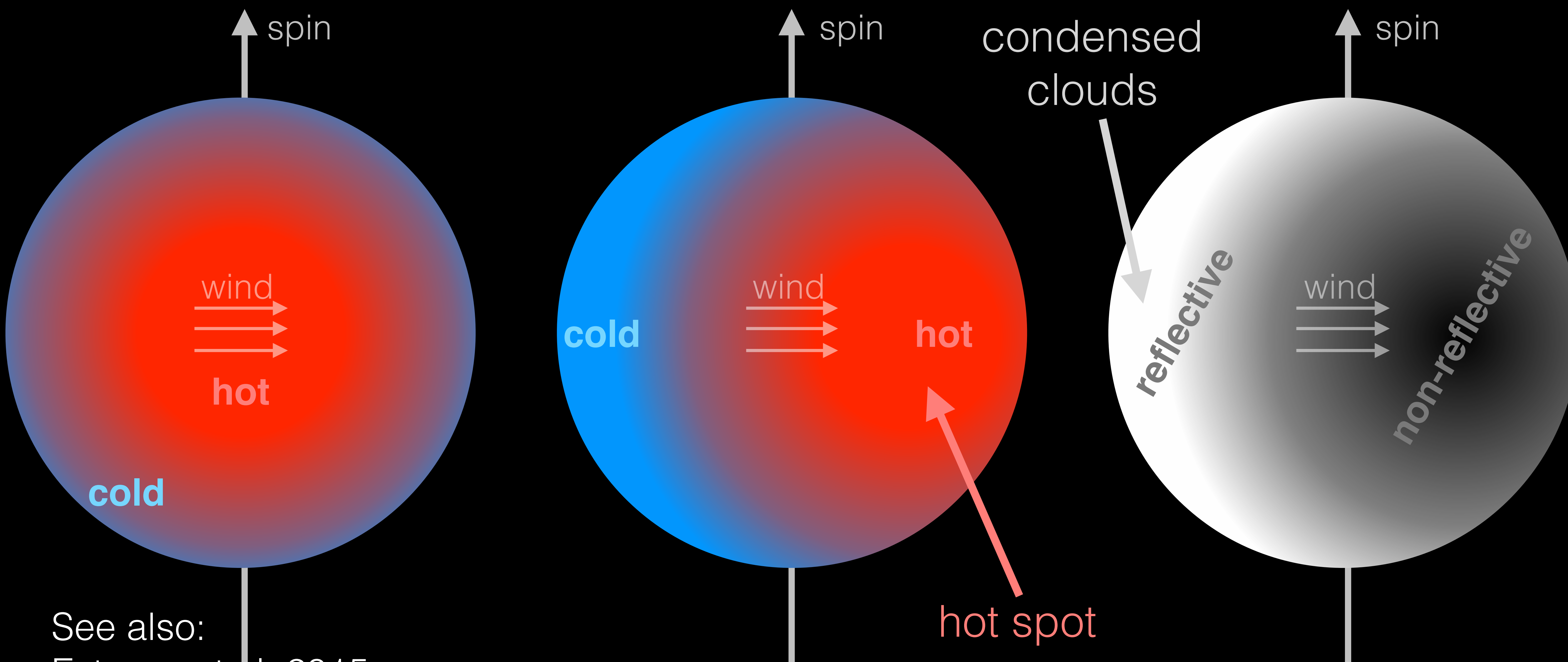

See also:
Esteves et al. 2015,
Faigler & Mazeh 2015

Thermal image

Reflected light image

Atmosphere-dominated *kepler* phase curves

Shporer & Hu 2015

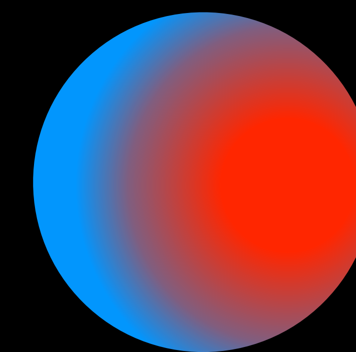

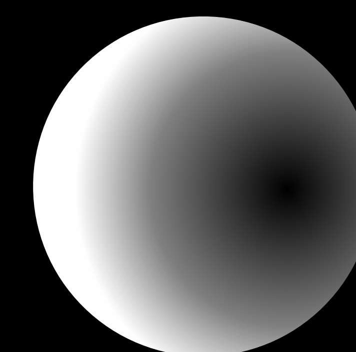

Take-home message:

Post-occultation phase max, reflection “bright spot”

Phase shifts in hot-Jupiters are common

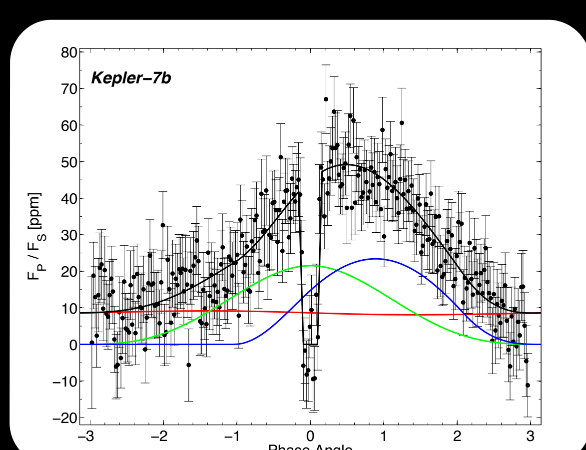

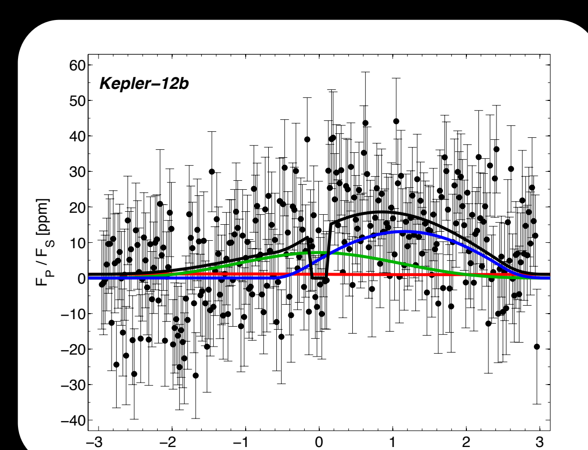

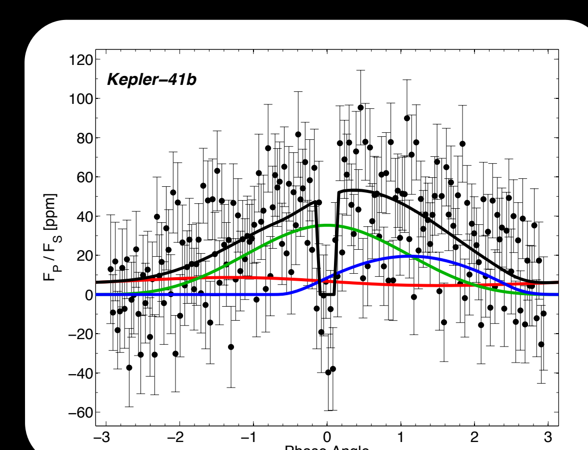

Two-Front Effort

Detailed study:
- Atmosphere
- Ellipsoidal distortion

Orbital phase curves

Detection Method, rare systems:
- Non-eclipsing
- Large sample

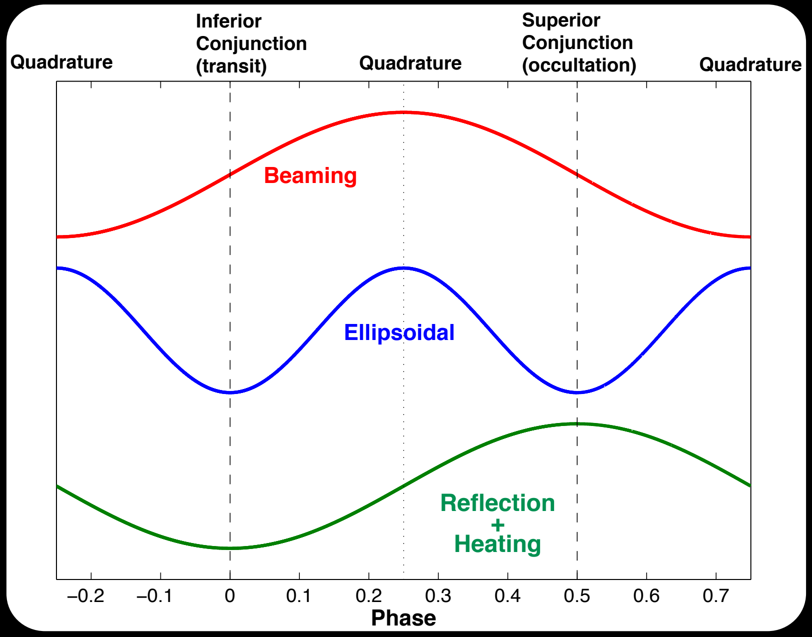

Kepler Beaming Binaries @ WIYN/Hydra

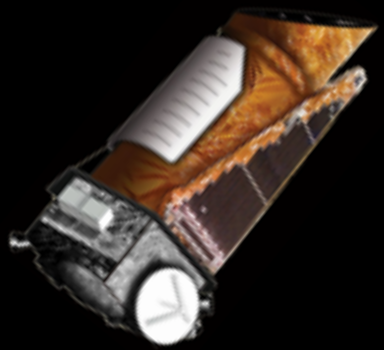

Collaborators: Keivan Stassun, Tabby Boyajian, Simchon Faigler, Tsevi Mazeh, Lev Tal-or, Andrej Prsa

Photometric detection → Radial velocity confirmation

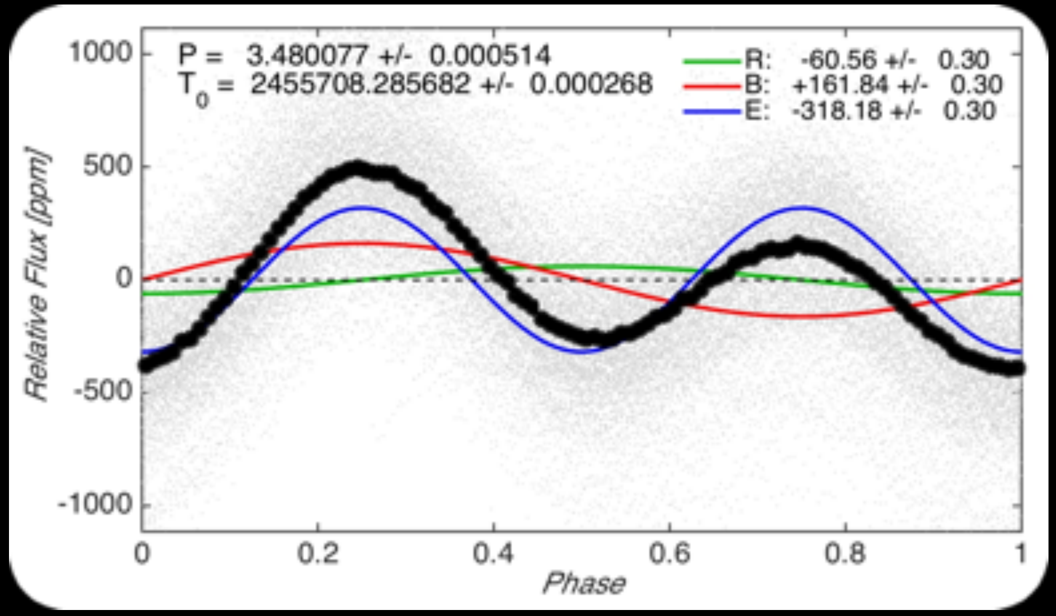

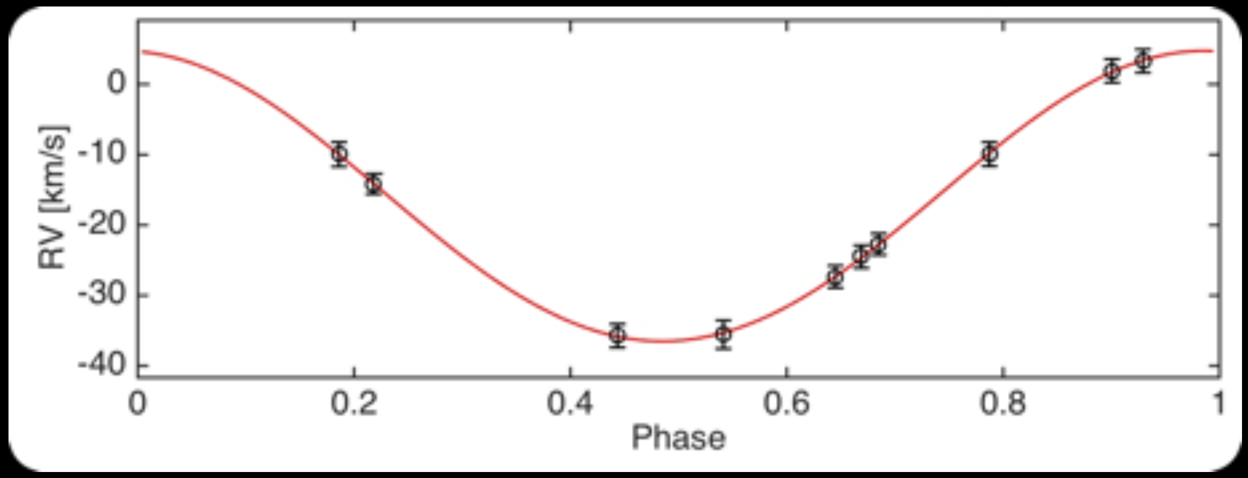

Now accepting cool project name suggestions…

WIYN/Hydra

Multi-fiber spectrograph

- 1.0 deg diameter
- Up to 90 fibers

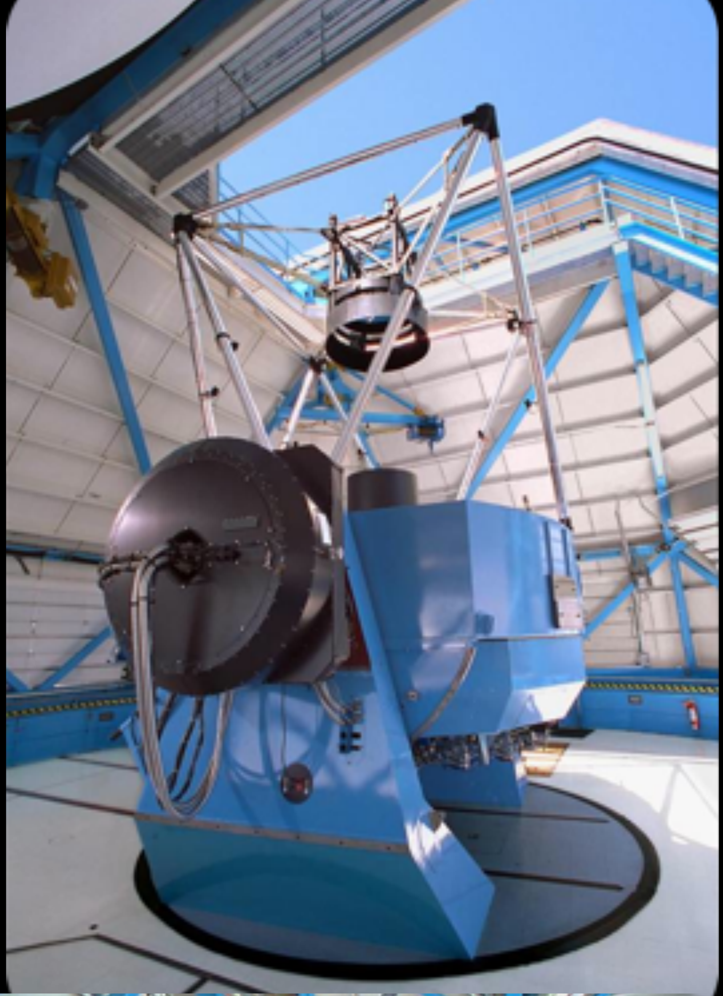

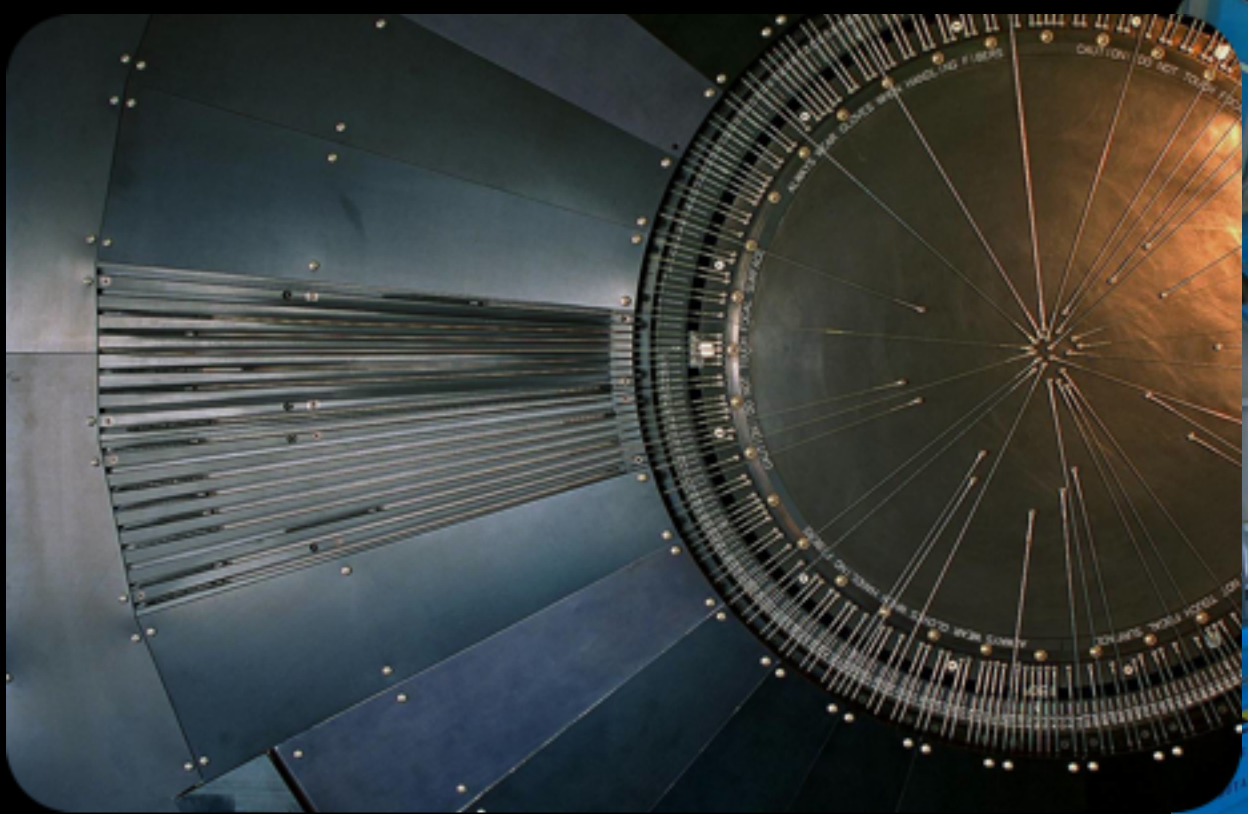

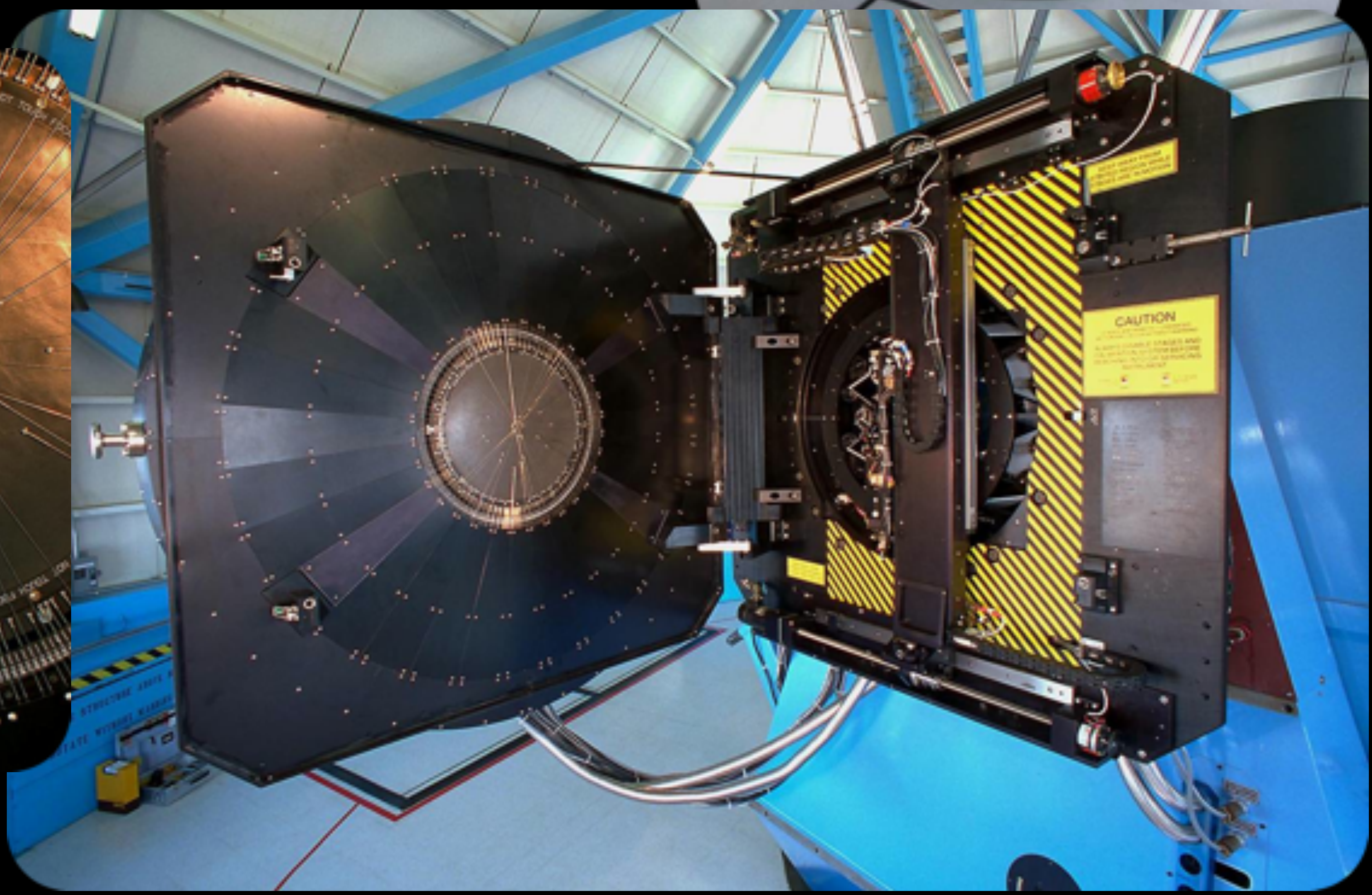

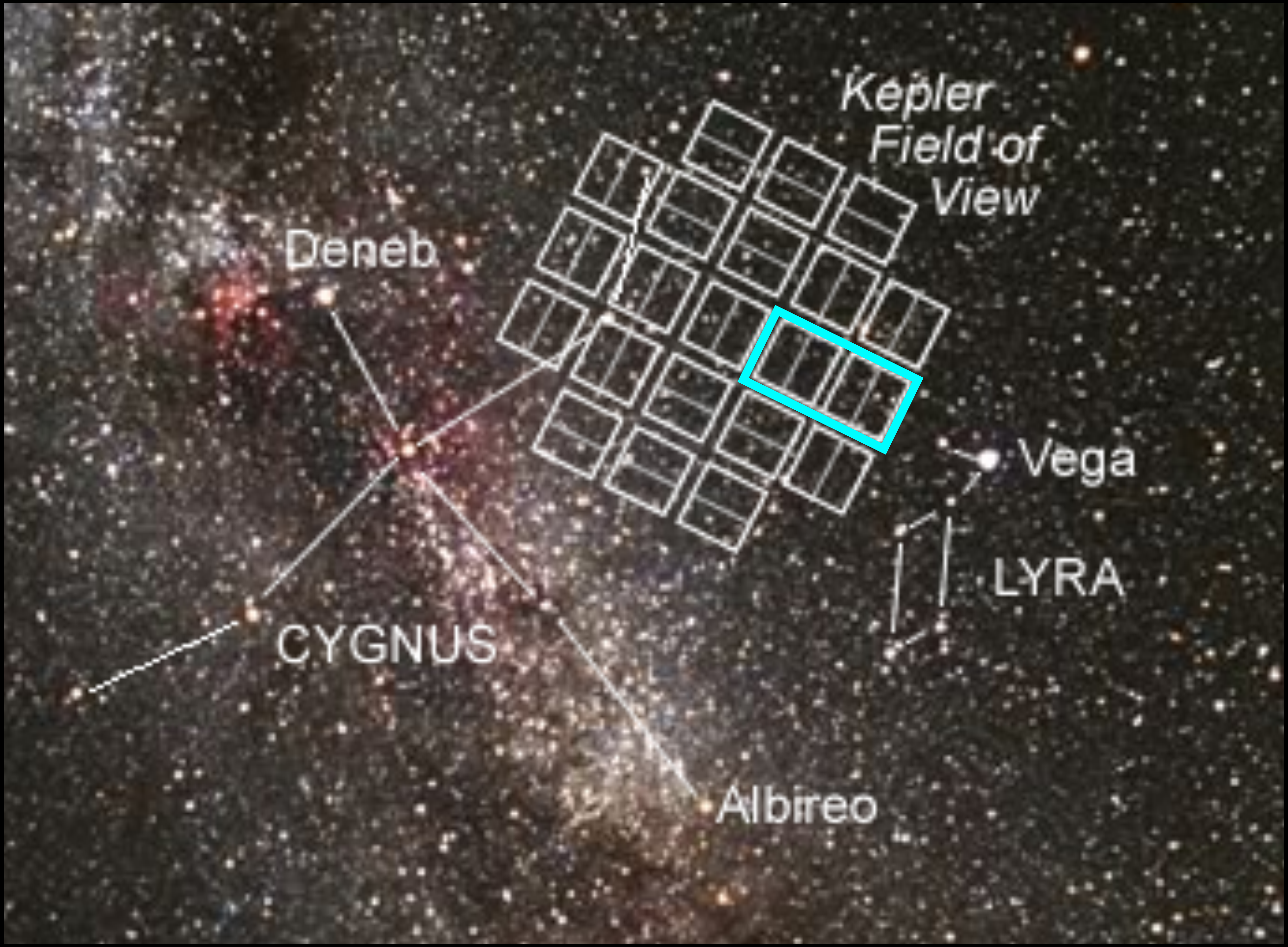

Kepler
Field of
View
Deneb
Vega
LYRA
CYGNUS
Albireo

Warning: Work in progress

Kepler Beaming Binaries @ WIYN/Hydra

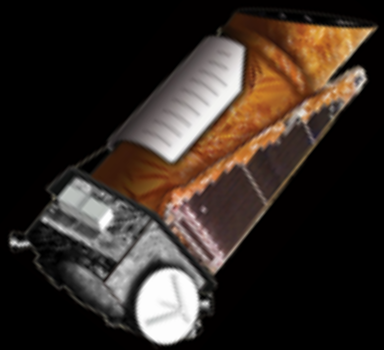

Future work:

- SB2
- Stellar spectral parameters
- Photometrically-predicted vs. RV-measured M_2
- Orbital modulations of eccentric systems
- Heartbeat stars

2015A: 9.5 nights

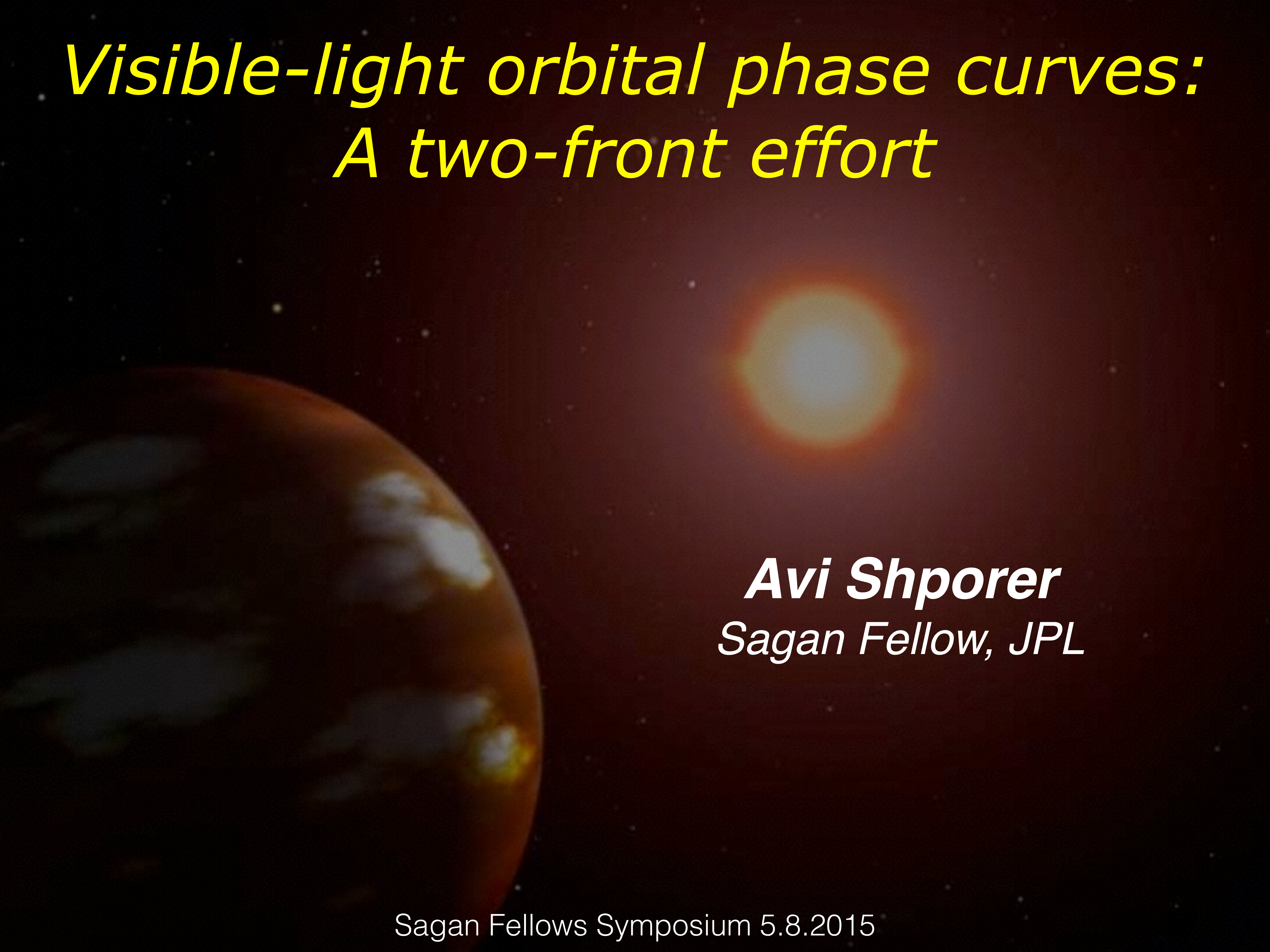

Visible-light orbital phase curves: A two-front effort

Avi Shporer
Sagan Fellow, JPL

Sagan Fellows Symposium 5.8.2015

EXTRA SLIDES

The Beaming Effect
aka Doppler Boosting

- Aberration
- Arrival rate
- Doppler shift

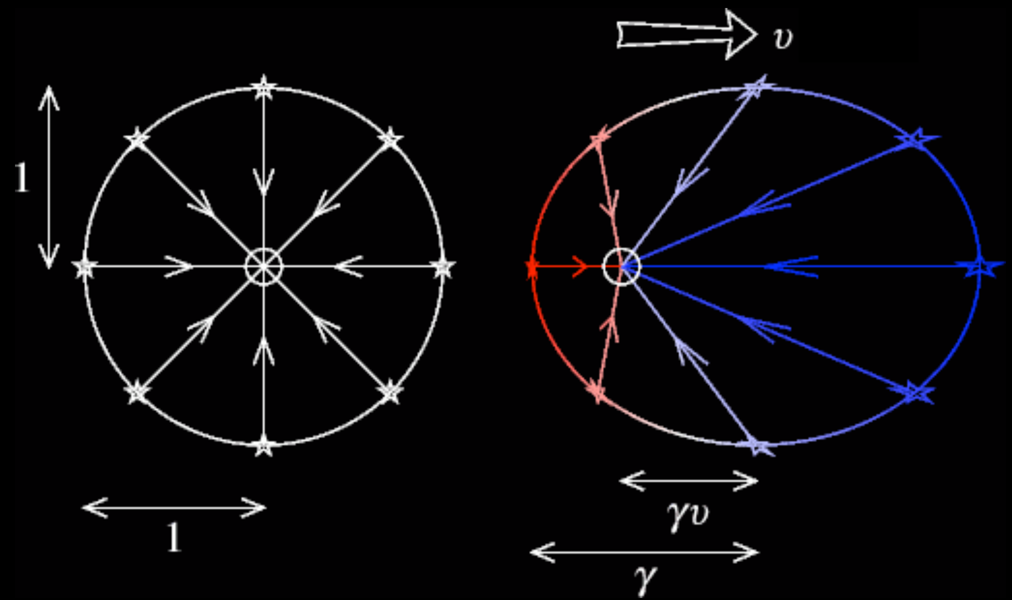

$$F_\nu = F_{\nu 0}[1 + (3-\alpha)\frac{v_r}{c}]$$

$$v_r \ll c$$

$$\alpha \equiv \frac{d \log F_\nu}{d \log \nu}$$

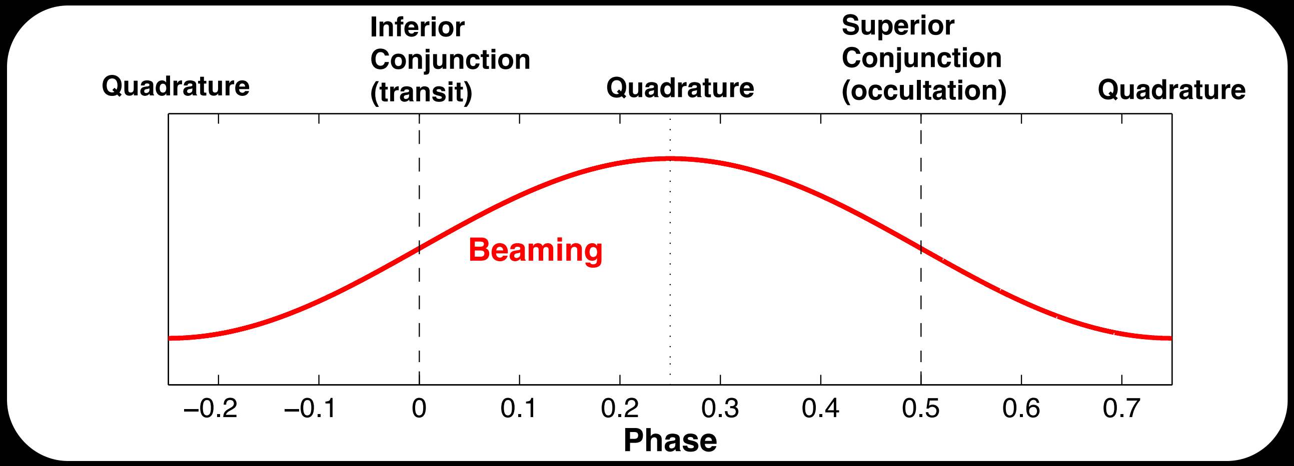

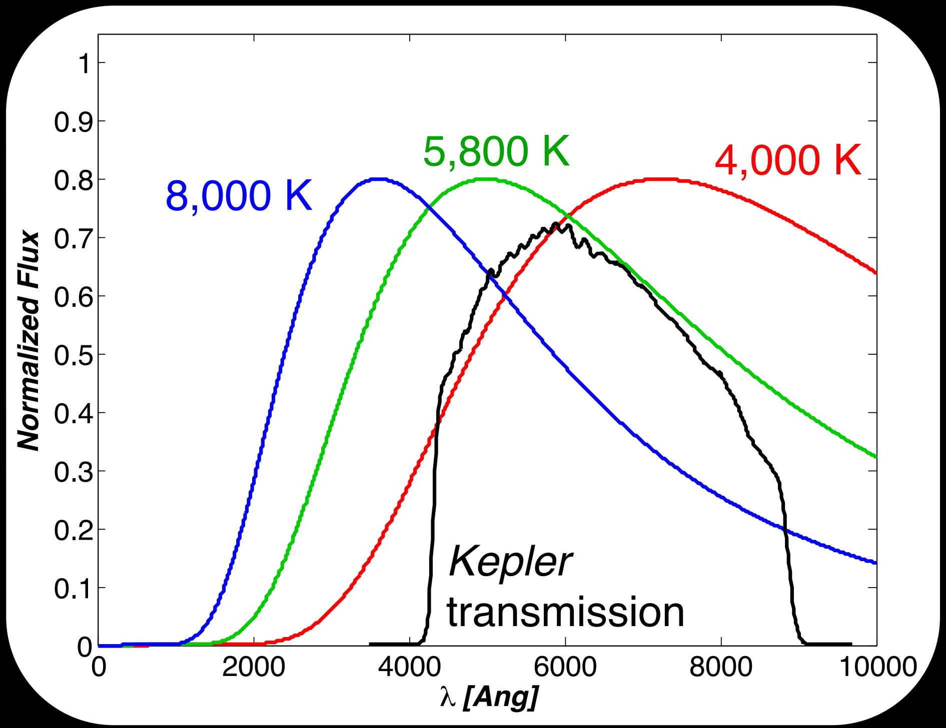

The Beaming Effect
aka Doppler Boosting

radial velocity variation ⇨ variation in observed flux

Photometric variation following orbital motion

$$A_{\rm beam} = \alpha_{\rm beam} 4 \frac{K_{RV}}{c}$$

bolometric $\alpha_{\rm beam} = 1$

$$A_{\rm beam} = 2.7\ \alpha_{\rm beam} \left(\frac{M_s}{M_{sun}}\right)^{-2/3} \left(\frac{P_{orb}}{\rm day}\right)^{-1/3} \left(\frac{M_2 \sin i}{M_J}\right)\ \rm ppm$$

Tidal Ellipsoidal Deformation

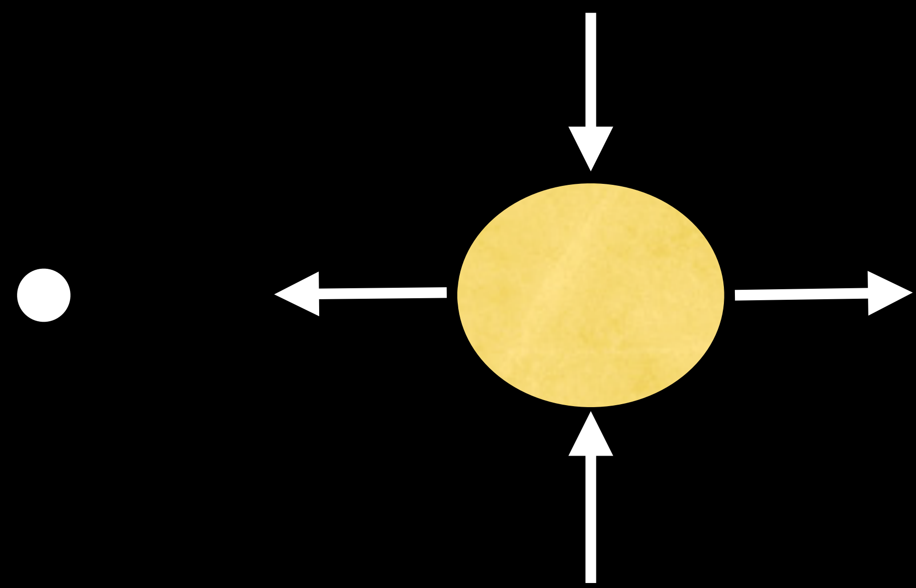

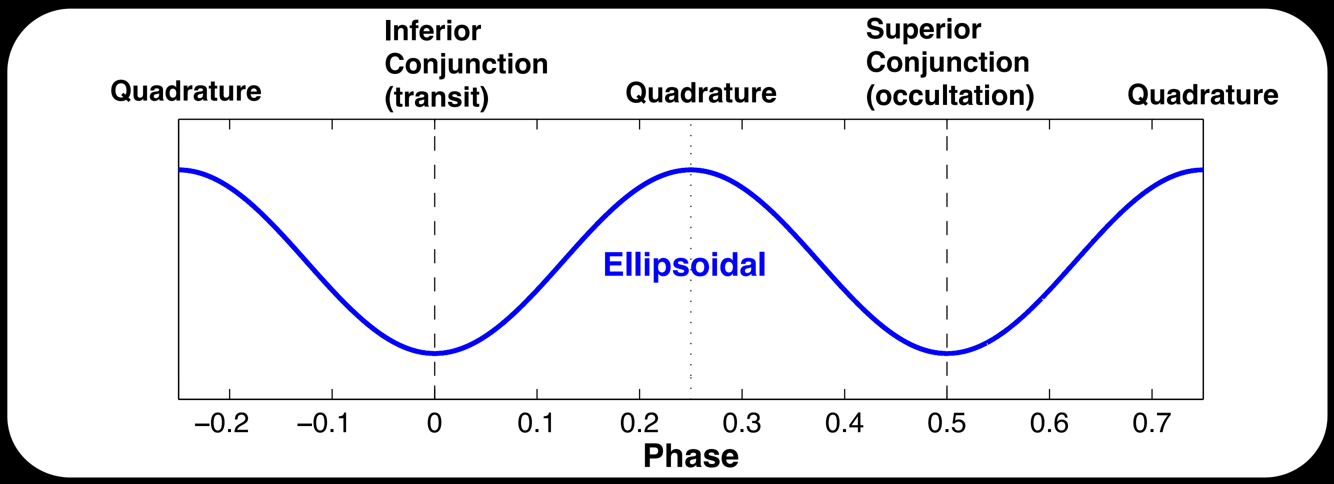

$$A_{\rm ellip} = \alpha_{\rm ellip} \frac{M_2 \sin i}{M_s} \left(\frac{R_s}{a}\right)^3 \sin i$$

$$A_{\rm ellip} = 13\ \alpha_{\rm ellip} \sin i \left(\frac{R_s}{R_{sun}}\right)^3 \left(\frac{M_s}{M_{sun}}\right)^{-2} \left(\frac{P_{orb}}{\rm day}\right)^{-2} \left(\frac{M_2 \sin i}{M_J}\right) \ {\rm ppm}$$

$$\alpha_{\rm ellip} = 0.15 \frac{(15+u)(1+g)}{3-u}$$

gravity darkening

limb darkening

Atmospheric: Reflection + Heating

$$A_{\rm refl} = \alpha_{\rm refl} 0.1 \left(\frac{R_2}{a}\right)^2 \sin i$$

$$A_{\rm refl} = 57\ \alpha_{\rm refl} \sin i \left(\frac{M_s}{M_{sun}}\right)^{-2/3} \left(\frac{P_{orb}}{\rm day}\right)^{-4/3} \left(\frac{R_2}{R_J}\right)^2\ \rm ppm$$

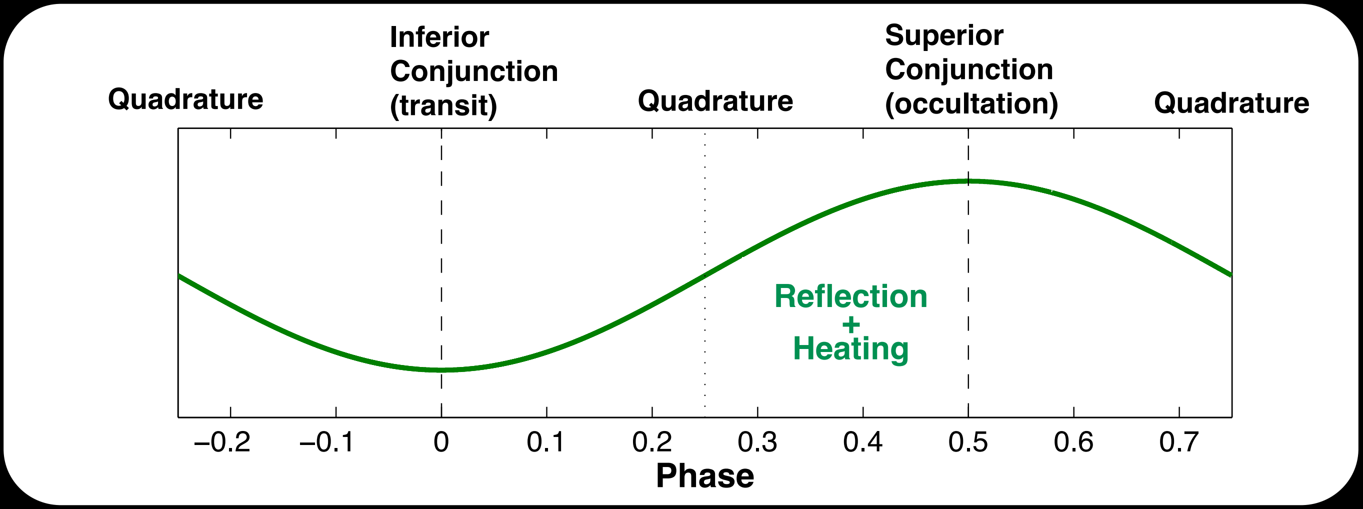

HYDRA POSITIONER CHARACTERISTICS	
Full Unvignetted Field Size	60 arc-minutes diameter
Minimum Fiber to Fiber Separation	37 arc-seconds
Positioning Accuracy	0.3 arc-seconds (30μm) rms measured
Configuration Time (100 fibers)	20-25 minutes
Total Number of Fiber Slots	288
Number of Guide Fibers (FOPs)	10 (two of the 12 now broken)
Number of Available Science Cables	2
Number of Active Fibers Per Cable	90 Red[2], 83 Blue[2]
Fiber Cable Length	25 meters
Blue Cable Spectral Window[1]	3000Å – 7000Å
Blue Cable Fiber Diameter	3.1 arc-seconds (310μm)
Red Cable Spectral Window[1]	4000Å – 1.8μm
Red Cable Fiber Diameter	2.0 arc-seconds (200μm)

From Hydra manual, p. 4
See also: http://www.wiyn.org/Instruments/wiynhydra.html